Liquid Crystals
Publication details, including instructions for authors and subscription information:
http://www.informaworld.com/smpp/title~content=t713926090

Studies on thermotropic liquid crystalline polyphosphates containing photoreactive dual mesogens

K. Rameshbabu[a]; P. Kannan[a]; R. Velu[b]; P. Ramamurthy[b]
[a] Department of Chemistry, Anna University, Chennai-600 025, India [b] National Center for Ultrafast Processes, University of Madras, Taramani, Chennai-600 113, India

To cite this Article Rameshbabu, K. , Kannan, P. , Velu, R. and Ramamurthy, P.(2005) 'Studies on thermotropic liquid crystalline polyphosphates containing photoreactive dual mesogens', Liquid Crystals, 32: 7, 823 — 832
To link to this Article: DOI: 10.1080/02678290500191261
URL: http://dx.doi.org/10.1080/02678290500191261

Liquid Crystals, Vol. 32, No. 7, July 2005, 823–832

Studies on thermotropic liquid crystalline polyphosphates containing photoreactive dual mesogens

K. RAMESHBABU†, P. KANNAN*†, R. VELU‡ and P. RAMAMURTHY‡

†Department of Chemistry, Anna University, Chennai-600 025, India

‡National Center for Ultrafast Processes, University of Madras, Taramani, Chennai-600 113, India

(*Received 10 January 2005; accepted 21 April 2005*)

A series of thermotropic liquid crystalline polyphosphates, containing photochromic molecules of stilbene in the backbone and substituted azobenzene in the side chain, were synthesized respectively. The inherent viscosity measurements were determined for all the polymers. The stability and char yield, T_g, T_m and T_i were investigated by thermal analysis. Polarizing optical microscopy of all the polymers exhibited birefringent melts with liquid crystalline behaviour. Variable temperature powder X-ray diffraction techniques were performed for confirmation of textures. UV-visible photolysis studies investigated the simultaneous behaviour of reactivity rates of crosslinking of stilbene units and isomerization, caused by azobenzene units in the main chain/side chain LCPs. Photoisomerization kinetics demonstrated the switching time rates for the *trans-cis* conversion of the azobenzene unit. A model polymer was synthesized and compared for the effect of stilbene in the main chain. Dipole moment values were calculated for the simulated low molecular mass of the pendant substituents to predict the polarity using MOPAC 3D Pro.

1. Introduction

Liquid crystalline polymers (LCPs) are of increasing interest for their distinctive role in biomimetic behaviour and optoelectronic applications [1, 2]. On account of their excellent optical and thermal properties, both thermotropic main chain liquid crystalline polymers (MC-LCPs) and side chain liquid crystalline polymers (SC-LCPs) have attracted scientific and industrial interest [3–5]. However, only limited information has been available on structure–property relationships in the combined thermotropic LCPs. Stilbene, azobenzene and their derivatives have been extensively studied for their nonlinear optical properties [6] and photorefractivity [7]. Stilbenes are important synthetic precursors and have been successfully used as probes to investigate molecular environments. Their structure is useful because fluorescence and isomerization properties are strongly influenced by the surrounding matrix [8]. An interesting feature of the stilbenoid moiety is its effect on light, from which has emerged applications in optical brighteners, laser dyes [9], photoresists [10], photochemically crosslinked polymers [11] and many other areas [12]. The study of the stilbene and azobenzene moieties may have a substantial role in these emerging and challenging technologies. Azobenzene-containing polymers have been studied because of their potential application in the fabrication of devices in, for example, optical data storage, optical switching, photonics and fibre optic communications [13–16].

The incorporation of phosphate groups in the backbone has led to increased attention due to the increase in polarity and flame retardancy of the polymers. Moreover, organophosphorus polymers display attractive plasticizing properties and good thermal stability [17]. For the first time, we introduce the phosphate units at the intercept points between two non-identical mesogens. The combination of photoreactive non-identical mesogens (photocrosslinkable and nonlinear) were hitherto unreported in the literature, to the best of our knowledge.

In continuation of earlier research [18–20], this article describes the synthesis and photoresponsive character of combined LC polyphosphates containing photoreactive dual mesogens, namely stilbene and azobenzene, in the main chain and side chain respectively. The simultaneous occurrence of crosslinking and isomerization may be seen in solutions of the two components. This approach leads to the development of unique dual functional polymeric photoreactive materials.

*Corresponding author. Email: pakannan@annauniv.edu

Liquid Crystals
ISSN 0267-8292 print/ISSN 1366-5855 online © 2005 Taylor & Francis
http://www.tandf.co.uk/journals
DOI: 10.1080/02678290500191261

2. Experimental

2.1. *Materials and methods*

Bromoacetaldehyde diethyl acetal, phenol, fluoroaniline, chloroaniline, bromoaniline, nitroaniline, toluidine and 4-methoxyaniline (Merck, Germany) were used as received. Diethyl ether, dichloromethane, glacial acetic acid, triethylamine, ethanol, methanol, ethylene glycol, and dimethylformamide were used as received from Sisco Research Laboratory (SRL, India). All solvents were purified and dried by usual methods before use [21]. Potassium carbonate, potassium iodide and sodium sulphate were purchased from Qualigens, India and used as received. The synthesis of monomers and polymers is illustrated in scheme 1.

2.2. *Preparation of Dihydroxystilbene*

Dihydroxystilbene was prepared from phenol and bromoacetaldehyde diethyl acetal. Concentrated

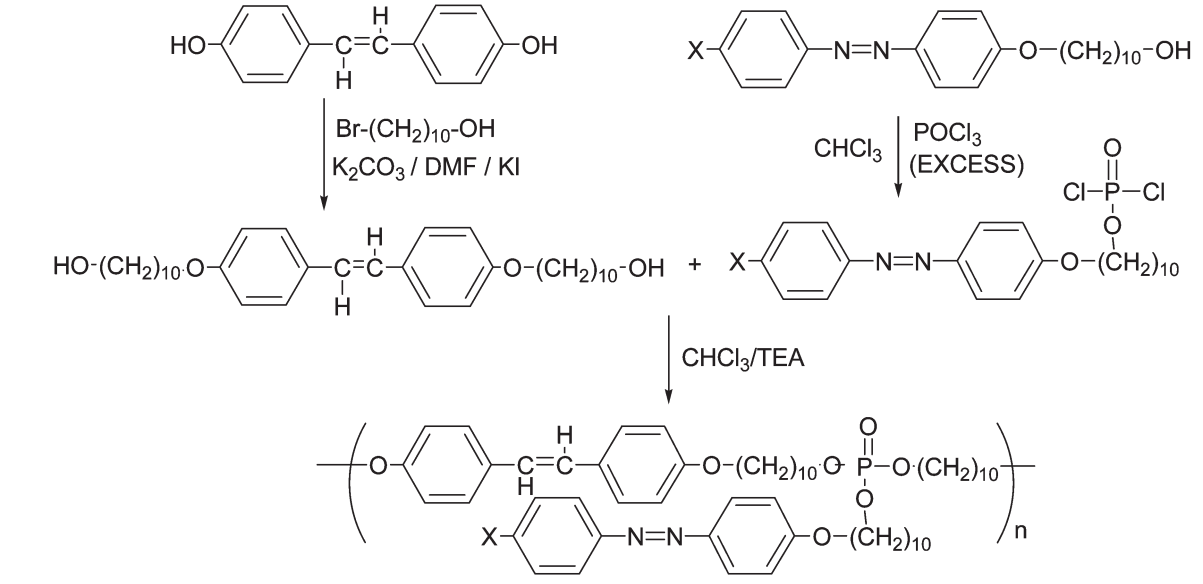

Polymer Name	PSAP-H	PSAP-F	PSAP-Cl	PSAP-Br	PSAP-CN	PSAP-NO_2	PSAP-CH_3	PSAP-OCH_3	PSAP-C_6H_5
X	H	F	Cl	Br	CN	NO_2	CH_3	OCH_3	Phenyl

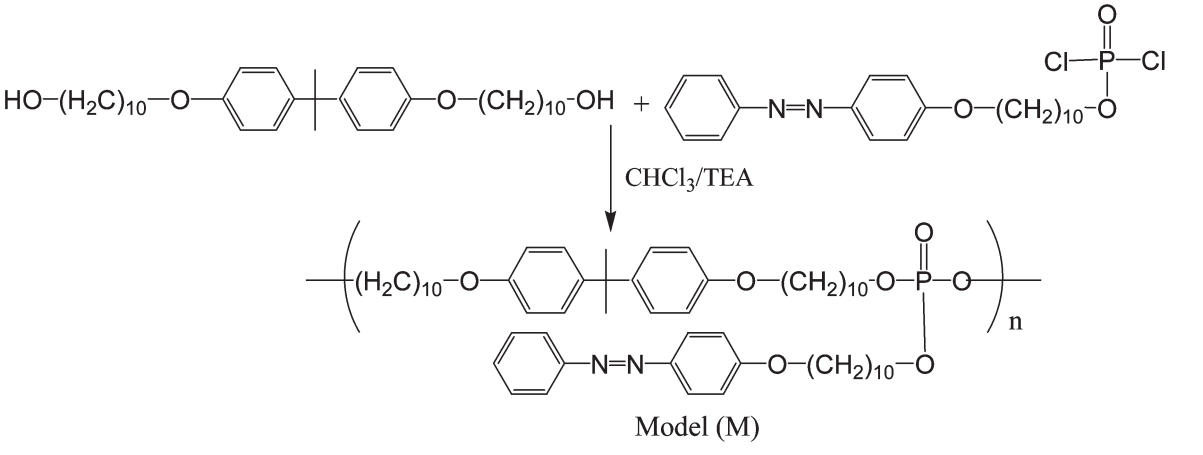

Model (M)

Scheme 1. Synthesis of the polymers.

sulphuric acid (25 ml) in glacial acetic acid (30 ml) was added dropwise with stirring during 1.5 h to a solution of phenol (0.12 mol) and bromoacetaldehyde diethyl acetal mixture (0.06 mol) in glacial acetic acid (150 ml) at 0°C. Stirring was continued at 0–3°C for 6 h. The concentrated solution was poured onto ice and extracted with diethyl ether. The ether extracts were washed with water, dried with sodium sulphate and distilled under reduced pressure below 35°C to obtain the condensation product.

Sodium (0.2 mol) was dissolved in methanol (500 ml) and ethylene glycol (250 ml). The mixture was distilled until the bulb temperature reached 190°C. The condensation product in ethylene glycol (100 ml) was then added dropwise under nitrogen to the hot sodium glycolate solution during 1 h; stirring was continued for 45 min at 190–195°C. The yellow fluorescent mixture was cooled to 60°C and poured into ice/water (1000 ml). On acidifying with 2N sulphuric acid (100 ml), the precipitated product was extracted with diethyl ether/acetone (7/3) and twice with diethyl ether. The extracts were washed with water and evaporated below 35°C. The remaining solid was boiled with diethyl ether (100 ml), filtered and washed with diethyl ether. Crystallization from acetic acid and ethanol mixture, gave pure 4,4′-dihydroxystilbene; yield 60%, m. p. 283°C (lit. 283–285°C). IR (KBr, cm^{-1}): 3450 (phenolic OH), 1690 (trans ethylene), 1471 (CH_2 stretch). ^1H NMR (DMSO-d_6,): δ=6.77 (d, 2H), 6.99 (s, C=C) 7.31 (d, 2H).

2.3. *Preparation of X-substituted azobenzene (X=H, F, Cl, Br, CN, NO_2, CH_3, OCH_3 ,C_6H_5)*

Aniline (*X*=H) (0.3 mol) dissolved in aqueous hydrochloric acid (water 100 ml, conc. HCl 25 ml) was cooled in an ice–salt freezing mixture with stirring. To this solution, cold $NaNO_2$ (0.5 mol) in 20 ml of water was added dropwise to maintain the temperature below 5°C. Meanwhile, phenol (0.3 mol) was added to 10% NaOH in 50 ml water. To the solution of sodium phenoxide, the diazotised solution was added dropwise at temperature below 5°C; stirring was continued for 1–2 h. The solution was then added to ice-cold water and neutralized with dil. H_2SO_4 solution to get obtain a crystalline product, which was filtered and dried in vacuum at 50°C. The product was recrystallized from chloroform to give the pure compound; yield 80%. ^1H NMR ($CDCl_3$,): δ=1.29 (m, CH_2), 3.94 (t, O–CH_2), 3.53 (t, CH_2–OH), 6.97 (d, phenyl attached to oxygen), 7.93 (d, 2H), 7.83 (d, 2H) 7.46 (m, 2H).

The other precursors were synthesized in the same way from the appropriately, substituted anilines [20].

2.4. *Preparation of monomers*

2.4.1. 4,4′-bis(10-Hydroxydecyloxy)stilbene. 4,4′-Dihydroxystilbene (0.05 mol) was dissolved in dry DMF (10 ml). Anhydrous potassium carbonate (0.05 mol) and 5 wt % of potassium iodide were added, and the mixture was heated to 90°C with constant stirring, 10-Bromodecanol (0.1 mol) was added dropwise to the reaction mixture and reaction continued for two days. The reaction mixture was then cooled to room temperature and poured into ice-cold dilute hydrochloric acid. The precipitated product was filtered, washed with water until neutral and then dried *in vacuo*; yield 62%. IR (KBr, cm^{-1}): 1425 (C–O stretch), 1550 (ethylenic linkage), 1950 (Ar CH_2), 2924 (CH_2 stretch), 3450 (phenolic OH). ^1H NMR ($CDCl_3$): δ=1.24 (s, CH_3), 4.9 (S, *trans* ethylene), 7.09 (m, aromatic *ortho* to CH), 6.95 (d, aromatic *ortho* to CH_3), 6.73 (d, 2H aromatic *meta* to CH), 6.68 (d, 2H, aromatic *meta* to C–CH_3).

2.4.2. 4-*X*-Substituted phenylazo-4′-phenyloxydecyl-phosphordichidates (X=F, Cl, Br, CN, NO_2, CH_3, OCH_3, C_6H_5). 4-(10-Hydroxydecyloxy)-4′-*X*-substituted azobenzenes were prepared by reacting *X*-substituted azobenzene with 10-bromodecanol, using a similar procedure to that adopted for the synthesis of 4,4′-bis(10-hydroxydecyloxy)stilbene; yields 85–90%.

4-(10-Hydroxydecyloxy)azobenzene (0.02 mol) was dissolved in dry chloroform (25 ml) and freshly distilled phosphorus oxychloride (0.04 mol) added. The reaction mixture was slowly heated to 50°C with constant stirring over one hour and then raised to reflux conditions. The reaction was continued until HCl evolution ceased. Excess phosphorus oxychloride was distilled off under reduced pressure and the residue connected to high vacuum for several hours. The reddish brown solid thus obtained was used immediately for the polymerization reaction without further purification. A small amount of phosphorodichloride monomer was heated under reflux with methanol (50 ml), and the incorporation of the phosphorus unit confirmed spectroscopically. All other 4-(X)-substituted phenylazo-4′-phenyloxydecyl phosphorodichloridates were prepared in a similar manner [20].

2.5. *Polymerization*

All the polymers were prepared by solution polycondensation at room temperature using triethylamine (TEA) as acid scavenger. The typical methodology for the preparation of polymer PSAP-H is as follows. 4,4′-bis(10-Hydroxydecyloxy)stilbene (0.05 mol) was dissolved in dry chloroform (20 ml). Dry triethylamine

(0.1 mol) was added under nitrogen with stirring at room temperature. To this reaction mixture, 4-phenylazo-4′-phenyloxydecyl phosphorodichloridate (0.05 mol) dissolved in chloroform was added dropwise over a period of 30 min. During the addition, the solution became homogeneous, and the reaction continued for 24 h. The reaction mixture was heated under reflux for a further 2 h and the concentrated solution poured into excess methanol. The colored precipitate thus formed was filtered and dried at 50°C under vacuum for 24 h. The purity of the polymers was examined by FTIR and ^{1}H NMR spectroscopy. All other poly(bis-4,4′-stilbeneoxy-4-X-substituted phenylazo-4′-phenyloxydecylphosphate ester)s (PSPA-*X*) were prepared by similar methods. A model polymer was prepared by reacting 4,4′-bis(10-hydroxydecyloxy) diphenylisopropylidene with 4-phenylazo-4′-phenyloxydecylphosphorodichloridate in a similar manner. PSAP-H: IR (KBr, cm^{-1}): 1262 (Ar–O–C), 1244 (P=O), 1588 (C=C), 763 (P–O), 1500 (N=N), 3441 (P–OH), 2924 (CH_2). ^{1}H NMR ($CDCl_3$): δ=1.66 (s,=CH alpha CH_3), 6.7 (s, *trans* ethylene), 7.4 (d, *ortho* to aromatic=CH), 7.2 (d, aromatic *ortho* to –CH_3), 6.9–7.0 (d, aromatic *ortho* to O–CH_2), 4.0 (m, aromatic O–CH_2), 1.29, 1.55 (m, O–CH_2), 6.5 (d, azo aromatic *ortho* to O–CH_2), 7.8 (d, azo aromatic *meta* to O–CH_2).

2.6. *Characterization*

The inherent viscosity measurements were carried out with an Ubbelohde viscometer thermostated at 30°C. In each case a solution of 100 mg of related polyphosphates in $CHCl_3$ was used for measurements. High resolution ^{1}H NMR spectra were recorded on Perkin Elmer and Varian 300 MHz spectrometers, respectively. ^{31}P NMR spectra were recorded on a JOEL 300 MHz NMR instrument with triphenylphosphine as an external standard with dual (^{31}P/^{1}H) probe. Thermogravimetric analysis (TGA) thermograms were recorded on a Mettler Toledo (USA) STAR^e system under a nitrogen atmosphere. The heating rate for TGA was 20°C min^{-1} with a nitrogen flow of 20 ml min^{-1} to determine the stability, decomposition and char yield. The phase transitions were determined by the endotherm heating rate using a Mettler Toledo (USA) STAR DSC at a scanning rate of 20°C min^{-1} with a nitrogen flow of 20 ml min^{-1}.

Polarizing optical microscopy (POM) studies were performed with a Euromax polarizing microscope fitted with a Linkam HFS 91 heating stage and a TP-93 temperature programmer. Samples were placed between two thin glass cover slips and melted with heating and cooling at 2°C min^{-1}. Photographs were taken with a Nikon FM10 camera and printed on Konica 400 film. All the photomicrographs were taken during the second cooling stage from isotropic transition to melting temperature. Powder X-ray diffractograms were recorded on a Rigaku Miniflex powder diffractometer equipped with a Guiner camera, using nickel-filtered CuK_α radiation, 40 kV voltage, 30 mA electric current, a scanning rate of 5°C min^{-1} and a scanning range of 0°–30°. The polymer was heated to 320°C in regular temperature intervals of 40°C and observations made at each interval.

Photocrosslinking and isomerization studies of all the polymers were carried out using a low pressure UV lamp (Spectroline Pencil lamp, New York) irradiating at 365 nm wavelength. The intensity of light reaching the dichloromethane was measured to be 3.04×10^{15} photons s^{-1}. The polymer was dissolved in dichloromethane solution (4.0×10^{-5} mol l^{-1}) in a 1 cm Quartz cuvette and irradiated for 1 min; the UV-visible absorption of the solution was measured immediately on a UV-vis spectrophotometer (Agilent 8453 Japan). The experiment was repeated until reduction in absorbance was complete. Dipole moment values were calculated for the simulated low molar mass of the SC pendant substituents using MOPAC 3D pro.

3. Results and discussion

3.1. *Synthesis*

The 4,4′-dihydroxystilbene was synthesized using a condensation reaction [22]. Under Williamson's ether conditions, 4,4′-bis(10-hydroxydecyloxy)stilbene was prepared by reacting dihydroxystilbene with 10-bromo-1-decanol in the presence of DMF with a catalytic amount of potassium iodide (scheme 1). In a similar manner, 4-X-substituted-4′-hydroxyazobenzene (*X*=H, F, Cl, Br, CN, NO_2, CH_3, OCH_3, C_6H_5) was prepared and alkylated. The alkylated azobenzene derivatives were reacted with excess of phosphorus oxychloride to give the corresponding substituted (*X*=H) azobenzeneoxydecylphosphorodichloridates, which were used without further purification for the polymerization reaction. The polymers were prepared by the solution polycondensation method at room temperature, with the reaction time increased to 2 h under reflux, then concentrated. Inherent viscosity of the polymers was measured in chloroform solution at 30°C, with the results presented in table 1. The results show that the polymers have fairly high molecular masses. The ^{31}P NMR spectra of the polymers show two signals; the resonance signal corresponding approximately to −13.0 δ is due to the P in the main chain, and the other signal at −6.5 δ is the P at the chain ends, which confirms

Table 1. Polymerization conditions, yields, inherent viscosity and λ_{max} for combined LCPs.

Polymer	Polymerization conditions Temp/°C, time/h	Yield/%	η/dl g^{-1}	λ_{max} (S)/nm	λ_{max} (A)/nm
PSAP-H	30(24)+60(3)	80	0.69	260	350
PSAP-F	30(24)+60(3)	78	0.76	234	375
PSAP-Cl	30(24)+60(3)	65	0.83	240	386
PSAP-Br	30(24)+60(3)	72	0.75	238	364
PSAP-CN	30(24)+60(3)	78	0.85	262	345
PSAP-NO_2	30(24)+60(3)	60	0.68	264	398
PSAP-CH_3	30(24)+60(3)	72	0.79	243	346
PSAP-OCH_3	30(24)+60(3)	78	0.72	258	345
PSAP-C_6H_5	30(24)+60(3)	72	0.80	244	354
Model	30(24)+60(3)	68	0.60	–	386

S=Stilbene; A=Azobenzene

the incorporation of phosphorus into the polymer backbone.

3.2. *Thermal analyses*

TGA for all the polymers was obtained under nitrogen; thermograms for the range of polymers are depicted in figure 1. The temperature corresponds to the three-stage decomposition representing the fragmentation of all the polymers. The first two-stage cleavages may be attributed to the evolution of nitrogen from the side chain azo moieties and to the phosphate ester units linking the MC/SC of the polymers [23]. Finally, the third stage cleaved at the ether groups attached to the main chain. The thermal stability of the polymers was noted to be above 200°C. The char percentage of all the polymers at 600°C is in the range 23–38%. The char yield is highest for the phenyl-substituted polymer (PSAP-C_6H_5); this may due to the high aromaticity of the phenyl ring. On the other hand, the char yield is low for the chloro- and methyl-substituted polymers. In general, the electron-withdrawing substituent polymers showed higher char yield than those with an electron-donating substituent. The occurrence of relatively high char yields of carbonaceous matter may be attributed to the pyrolytic cleavage and fragmentation of LCPs to yield phosphoric acid as the final product [24] (see table 2). Transition temperatures from differential scanning calorimetry (DSC) are summarized in table 3

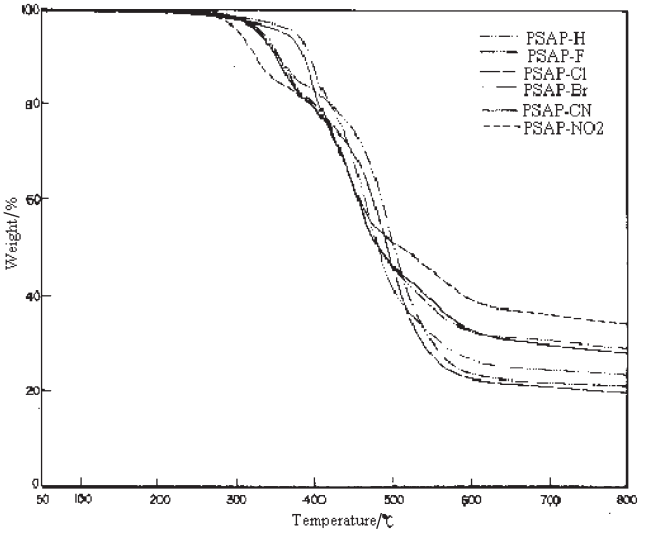

Figure 1. TGA plots of the polymers PSAP-H to PSAP-NO_2 in nitrogen at a heating rate of 10°C min^{-1}.

Table 2. TGA thermogram data of all the polymers for combined LCPs.

Polymer	Stages of decomposition temperature/°C I	II	III	Maximum weight loss at 600°C/%	Char yield at 600°C/%
PSAP-H	250	330	450	73	24
PSAP-F	260	360	498	65	35
PSAP-Cl	290	400	512	77	23
PSAP-Br	300	400	522	75	25
PSAP-CN	320	410	490	68	32
PSAP-NO_2	330	425	485	63	37
PSAP-CH_3	322	412	490	80	20
PSAP-OCH_3	318	423	523	68	32
PSAP-C_6H_5	320	428	510	62	38
Model	321	433	500	72	28

and thermograms are presented in figure 2. The DSC data were recorded during the second heating scan. The polymers exhibit an apparent softening point around 55°C, which seems fairly low because of the incorporation of the phosphorus unit and the terminal substituents of the SC mesogen. Melting transition temperatures (T_m) were obtained in the range 110–160°C. Isotropic transitions (T_i) occurred in the range 175–321°C. The wide temperature range between thermal transitions indicated a high stability of the mesophase. The mesophase range was higher for polymers with bromo, cyano and nitro substituents than the other polymers; this may be due to the size of the substituents. The principle effect of lengthening the flexible spacers was to decrease the transition temperature and to increase the mesophase range. These results agree with our prediction.

3.3. *Liquid crystalline properties*

All the polymers showed birefringent melts and exhibited LC behaviour under POM; representative photomicrographs of monomer precursors and the polymers PSAP-Br and PSAP-NO_2 are shown in figure 3. The monomers and polymers were sandwiched between cover slips, heated to the isotropic state, then slowly cooled. It is interesting to note that both the alkylated MC and SC precursors exhibited nematic LC behaviour. In the polymers, the textures of all the phases were observed during the first cooling cycle just below the isotropic transition temperature. The linking (azo) groups connect two aromatic core units and conjugation is extended over the longer molecule, enhancing the polarizibility anisotropy [25]. In the case of the SC terminal substituents (methyl, phenyl, methoxy, cyano and unsubstituted) the nature of these

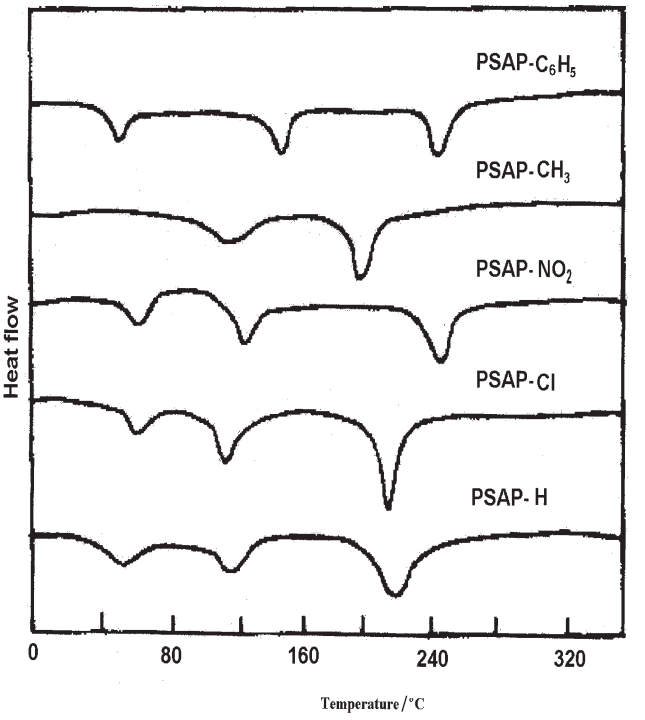

Figure 2. DSC thermograms of polymers PSAP-H, PSAP-Cl, PSAP-CN, PSAP-CH_3 and PSAP-C_6H_5.

groups leads to the possibility of unidentified smectic-like textures [26, 27]. The terminal substituent is important in size and in the nature of its polarity. Hence, the intermolecular interaction, dipole-induced dipole interactions play a vital role in determining the type of mesophase texture and influence the viscosity of the polymers. The characteristic texture of polymer PSAP-Br exhibited the anisotropic state of a smectic phase, whereas polymer PSAP-NO_2 exhibits the fine textures which coarsen on cooling. Polymers PSAP-CN

Table 3. DSC, POM and dipole moment data of the polymers.

	DSC/°C				POM/°C				
Polymer	T_g	T_m	T_i	ΔT	T_m	T_i[a]	ΔT[b]	Type of mesophase	D[c]
PSAP-H	55	118	220	102	120	214	94	Smectic	2.5
PSAP-F	—	120	230	110	122	225	103	Smectic	4.1
PSAP-Cl	60	110	216	106	115	210	95	Smectic	3.7
PSAP-Br	—	152	321	169	140	315	175	Smectic	3.5
PSAP-CN	60	125	243	118	124	240	116	Smectic	5.5
PSAP-NO_2	50	135	250	115	130	238	108	Smectic	8.8
PSAP-CH_3	—	120	190	70	118	186	68	Smectic	2.4
PSAP-OCH_3	58	160	240	80	155	231	76	Smectic	1.7
PSAP-C_6H_5	50	149	240	91	138	228	90	Smectic	2.5
Model	—	135	175	40	139	180	41	Nematic	2.0

[a]Ti observed only during the first heating cycle.
[b]ΔT=phase duration.
[c]D=dipolemoment values obtained from MOPAC 3D pro in Debye unit.

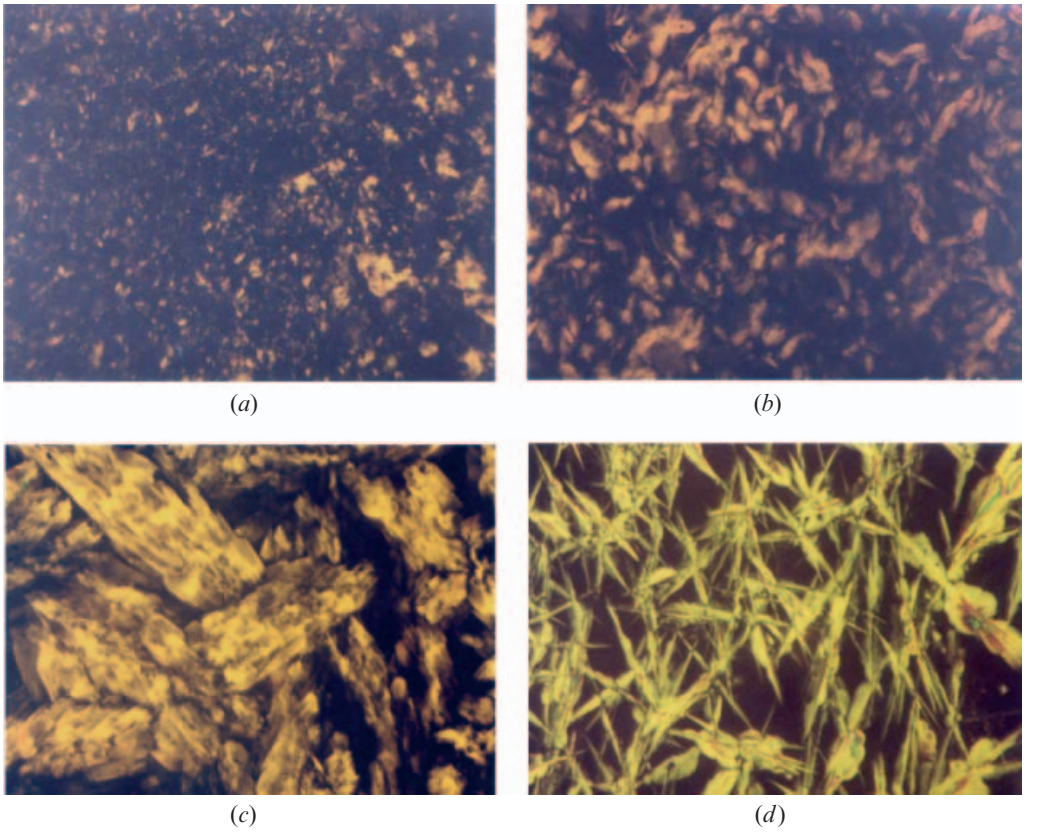

Figure 3. Typical POM photographs of monomers (MC-DHAMS and SC-chloro substituent): (*a*) at 140°C, (*b*) at 145°C; and polymers (*c*) PSAP-Br at 135°C, and (*d*) PSAP-NO_2 at 150°C, under crossed polarizers exhibiting LC phases (magnification 400X).

and PSAP-NO_2 exhibited more well defined textures than the other polymers. This is ascribed to the interaction of permanent and induced dipoles, which plays a significant role in these moieties [28]. It is worth noting to that the model polymer exhibits a lower order grainy nematic texture mesophase due to the incorporation of bisphenol-A in the backbone.

3.4. *X-ray diffraction Analysis*

X-ray diffraction (XRD) results from an unoriented sample of the bromo polymer PSAP-Br obtained at different temperatures are displayed in figure 4. The X-ray diagram shows a sharp reflection peak at low angle associated with smectic layers and a broad reflection at wide angle associated with lateral packing of the mesogens. The XRD pattern of the polymer shows a sharp peak at $2\theta=3.91^\circ$, corresponding to the periodic distance and the layer thickness 21.2 Å at 140°C, and 22.1 Å at 180°C. This suggests the layer characteristics of the smectic phase. The diffraction pattern indicates that the mesogenic rigid rods are arranged in layers. Thus, the bromo polymer exhibits the smectic LC phase [29]. A broad peak was found in the region $2\theta=17^\circ$–25°, classically due to lateral interference of the mesogenic cores with *d*-spacings of 4.0 Å at 140°C. On increasing the temperature above the isotropization the peak diminishes and the sample regains its original crystallinity on cooling.

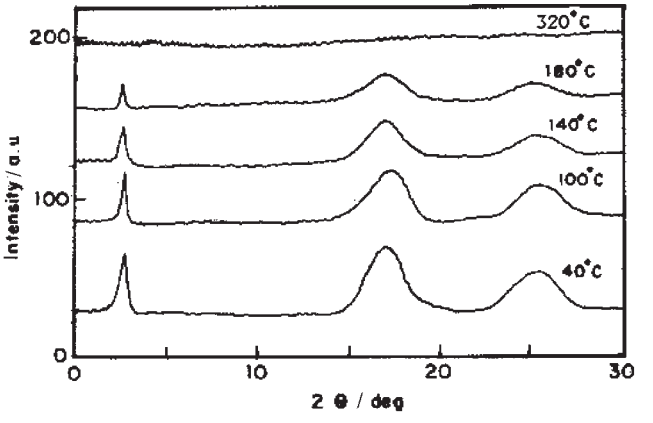

Figure 4. Variable temperature X-ray diffraction of polymer PSAP-Br. Scans observed between 40 and 320°C show a clear indication of phase transition (melting).

3.5. *Photolysis studies*

The UV-visible spectra for all the polymers, in dichloromethane solution, were quantitatively measured. The absorption maxima for the polymers containing MC stilbene are around 234 and 280 nm, while the maxima for SC azobenzene are observed at 375 and 430 nm, as shown in figure 5. The figure clearly shows the simultaneous observation of the crosslinking effect of the stilbene unit and the reversible back-reaction of the *cis–trans* isomerization process of the azobenzene unit [30, 31]. The representative relative rates of photocrosslinking of the polymers are shown in figure 6. The relative reactivity rate $(A_o\text{-}A_t/A_o)$ is plotted against the time t of irradiation, where A_o is the absorbance before irradiation and A_t is the absorbance after irradiation of time t. The intensity of the π–π* electronic transition of the *trans*-stilbene at 234 nm decreased in absorbance gradually, indicating the effect of dimerization of the olefinic double bond of the polymer chain, which involves the (2+2)π cycloaddition reaction leading to the formation of the cyclobutane ring. The crosslinking effects of the polymers were different in terms of time, and depend on the terminal substitution of the SC moiety. That the reactivity rate decreases with increasing optical intensity indicates the importance of mobility within the system. The order of the reactivity rate with substitution in the crosslinking is as follows: $OCH_3>NO_2>CN>Br>C_6H_5>Cl>F>H>CH_3$. It was found that after the end of irradiation (5 min) the system showed no further change. This may

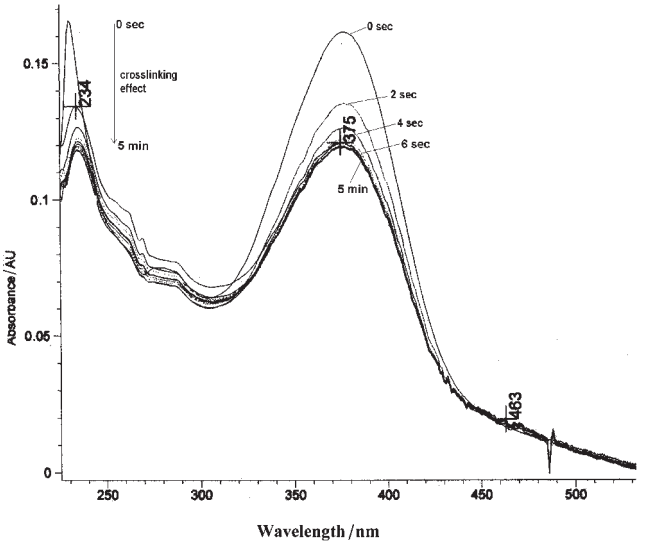

Figure 5. Simultaneous observation of absorption spectra of polymer PSDAP-F at different intervals of time: (*a*) 234 nm for crosslinking stilbene, (*b*) 375 nm for the stable *trans*-form of azobenzene, (*c*) 483 nm for the *cis*-form of azobenzene.

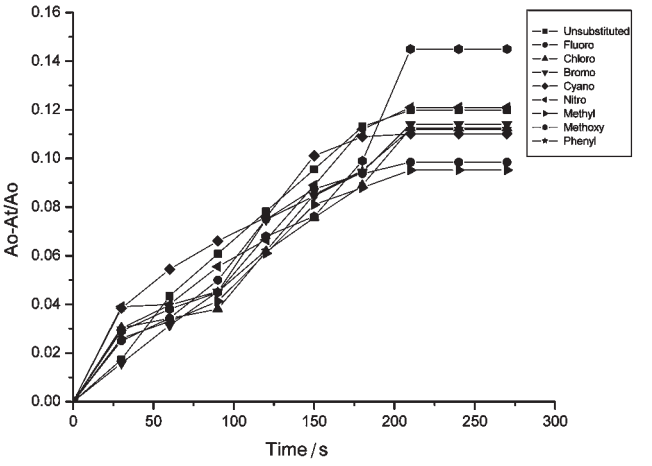

Figure 6. Reactivity rate of crosslinking caused by the stilbene unit of the polymers at different intervals of time.

be because the thermal back-reaction of stilbene is impaired indicating the presence of crosslinking [12].

However, for SC azobenzene the UV absorption spectrum in a dichloromethane solution of the cyano polymer (PSAP-CN) is observed at 350 and 425 nm for the *trans* and *cis* forms, respeclively. On irradiation of the cyano polymer solution, in analogy to the first π–π* transition, azobenzene chromophores undergo *trans–cis* photoisomerization. On substituting different terminal groups in the SC azobenzene moiety the shape, intensity and position of the UV absorption peak changes as shown in figure 7.

A model polymer was synthesized for comparison (see scheme 1). It included bisphenol-A in the MC and an azobenzene moiety in the SC, incorporated through the phosphate unit with a decamethylene spacer. A regular decrease in absorbance on irradiation for different intervals of time, and *trans–cis* isomerization were observed at 386 and 426 nm for SC moiety, as shown in figure 8. On comparing the model polymer with the MC stilbene unit using UV-vis spectroscopy, the structural variations and the influence of the SC mesogens are recognized. It is interesting to note that the completion of *trans–cis* isomerization took place in a shorter time for the dual chromophoric mesogen containing polymers than for the model polymer. This may be attributed to a faster response time or switching time for stilbene-containing polymers, which may be exploited in optoelectronic devices. The switching times taken for completion of *trans–cis* isomerization (photstationary state) are in the following order: $NO_2>CN>Br>OCH_3>Cl>F>CH_3>$Model$>C_6H_5>H$. It is recognized that the electron withdrawing groups are more highly polarizing than the electron-donating groups. Hence, the trends are well correlated with the

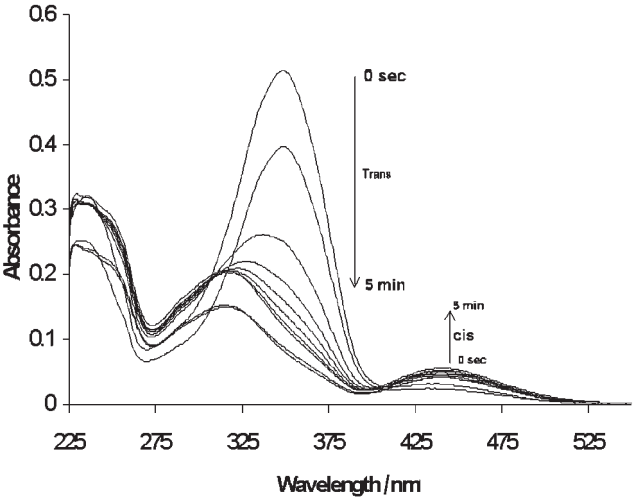

Figure 7. Absorption spectra of model polymer in comparison with MC-SC LCPs.

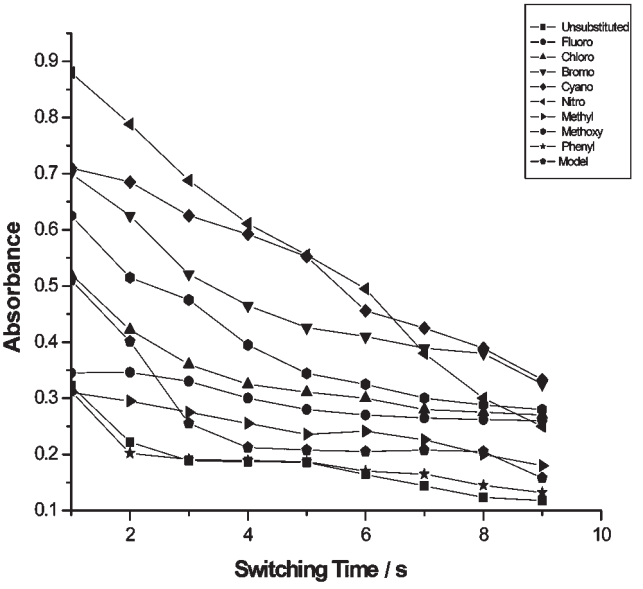

Figure 8. Photoisomerization of all the polymers at a concentration of 2×10^{-5} mol in dichloromethane observed at a wavelength of 375 nm caused by the *trans* form of azobenzene units.

reported theoretical dipole moment values and are calculated by the MOPAC 3D pro studies of all the different pendant substituents to predict the polare nature of the SC mesogen.

Based on these observations, it is clear that simultaneous occurrence of the crosslinking effect and the reversible isomerization process were seen in the dual photoreactive combined LCPs. The structural effect and switching behaviour of these molecules vary depending upon the size and dipolar nature of the SC pendant substituents. In the case of the model polymer, the MC does not act as a mesogen and it is bent shaped; the side chain azobenzene unit causes the isomerization.

4. Conclusion

A series of novel LC polymers containing both main (stilbene) and side (azobenzene) chain dual photoresponsive moieties were synthesized. Inherent viscosity values for all the polymers were calculated. Thermal stability and melting and isotropic transition temperatures were determined. The main chain and side chain monomers and all the polymers exhibited birefringent LC phases under POM observation. Variable temperature measurements confirmed the smectic phase textures. UV-vis photolysis studies demonstrated the crosslinking nature of the MC stilbene moiety and the reversible *cis–trans* isomerization of the photoreactive SC azobenzene moieties simultaneously. A comparison with the model polymer with stilbene unit in the MC, clearly confirms the crosslinking effect of the stilbene unit and the photoisomerization process caused by the azobenzene unit. The switching rate of the dual photochromic LCPs is shorter than that of the model polymer due to the isomerization of MC-SC mesogenic moieties. The combination of thermotropic liquid crystallinity and photolysis properties maker the polymers candidates for optoelectronic applications such as light emitting devices. The dipole moment values are in the range 2.0–8.8 D, as determined by MOPAC 3D Pro studies involving all the different pendant substituents. A fluorescence study of all the polymers is now in progress and will be continued in future work.

Acknowledgement

The authors thank the University Grants Commission, India (UGC No.F.12-113/2001, New Delhi, India) for financial support of this work. We are also grateful to Sophisticated Regional Instrumentation Center, Indian Institute of Technology, Chennai, India for spectral analysis.

References

[1] P.J. Collings, M. Hird. *Introduction to Liquid Crystals Chemistry and Physics*. Taylor & Francis, UK (2001).
[2] I.C. Khoo, S.T. Wu. *Optics and Nonlinear Optics of Liquid Crystals*. World Scientific, Singapore (1993).
[3] A. Cifferi (Ed.). *Liquid Crystallinity in Polymers. Principles and Fundamental Properties*. VCH, New York (1991).
[4] P.J. Collings, J.S. Pate (Eds). *Handbook of Liquid Crystal Research*. Oxford University Press, New York (1997).

[5] I.M.E. Ward. *Structure and Properties of Oriented Polymers*. Chapman & Hall, London (1997).
[6] G.H. Heilmeier, L.A. Zanoni. *Appl. Phys. Lett.*, **5**, 91 (1968).
[7] J. Zyss (Ed.). *Molecular Nonlinear Optics, Materials, Physics, and Devices*. Academic Press (1994).
[8] B. Meerholtz, L. Volodin Sandalphon, B. Kippelen, N. Peyghambarian. *Nature*, **49**, 371 (1994).
[9] D. Demus, J. Goodby, G.W. Gray, H.J. Weiss, V. Vill (Eds). *High Molecular Weight Liquid Crystals,* Vol. 3, p. 52, Wiley-VCH, New York (1998).
[10] R.A.M. Hikmet, B.H. Zwerver, J. Lub. *Macromolecules*, **27**, 6722 (1994).
[11] V. Ortiz, C.K. Ober, E.J. Kramer. *Polymer*, **39**, 3713 (1998).
[12] D. Blanc, S. Pelissier, K. Saravanamatu, S. Najafi, M. Andrews. *Adv. Mater.*, **11**, 1508 (1999).
[13] V. Cimrova, D. Neher, S. Kostromine, T. Bieringer. *Macromolecules*, **32**, 8496 (1999).
[14] R. Stockersman, P. Rocon. *Appl. Opt.*, **38**, 3714 (1999).
[15] C. Mcardle (Ed.). *Applied Photochromic Polymer Systems*. Blackie, London (1992).
[16] V. Shibaev, A. Bobrovsky, N. Boiko. *Prog. polym. Sci.*, **28**, 729 (2003).
[17] K. Kishore, P. Kannan, K. Iyanar. *J. polym Sci. A: polym. Chem.*, **29**, 1039 (1991).
[18] K. Rameshbabu, P. Kannan. *Liq. Cryst.*, **31**, 843 (2004).
[19] S. Senthil, P. Kannan. *J. polym. Sci. A: polym Chem.*, **40**, 2256 (2002).
[20] S. Kumaresan, P. Kannan. *J. polym. Sci. A: polym Chem.*, **41**, 3188 (2003).
[21] D.D. Perrin, W.L.F. Armarego. *Purification of Laboratory Chemicals,* 3rd Edn, Pergamon Press, New York (1988).
[22] K.B. Becker. *Synthesis*, 341 (1982).
[23] J.H. Lee, B.W. Jin, J.S. Jo, W.C. Kim, Y.S. Zin, Kang. *Acta. Polym.*, **50**, 399 (1999).
[24] S. Senthil, P. Kannan. *Liq. Cryst.*, **29**, 1297 (2002).
[25] P.J. Collings. *Liquid Crystals, Nature's Delicate Phase of Matter*. Princeton University Press, Princeton (1990).
[26] S. Friegberg, F.L. Labarthet, P. Rochon, A. Natansohn. *Macromolecules*, **36**, 2680 (2003).
[27] D. Demus, S. Diele, Grande, S. Sackmann. *Advances in Liquid Crystals*, G.H. Brown (Ed.), Academic Press, New York. pp. 1–85 (1983).
[28] G.W. Gray, P.A. Winsor. *Liquid Crystals and Plastic Crystals*. Ellis Harwood, Sussex, England (1974).
[29] T. Tasaka, V.F. Petrov, H. Okamoto, Y. Morita, K. Suetake, S. Takenaka. *Liq. Cryst.*, **29**, 1311 (2002).
[30] I. Dierking. *Textures of Liquid Crystals*. Wiley-VCH, Weinheim (2003).
[31] K. Ichimura. *Chem. Rev.*, **100**, 1847 (2000).